Accepted manuscript

Monitoring the curing process of epoxy adhesive using ultrasound and Lamb wave dispersion curves

Erwin Wojtczak, Magdalena Rucka

In: *Mechanical Systems and Signal Processing* 151, 107397

DOI: https://doi.org/10.1016/j.ymssp.2020.107397

Please cite this article as:

E. Wojtczak, M. Rucka, Monitoring the curing process of epoxy adhesive using ultrasound and Lamb wave dispersion curves, *Mechanical Systems and Signal Processing* 151 (2021), 107397, doi: https://doi.org/10.1016/j.ymssp.2020.107397

Monitoring the curing process of epoxy adhesive using ultrasound and Lamb wave dispersion curves

Erwin Wojtczak*, Magdalena Rucka

[1] Department of Mechanics of Materials and Structures, Faculty of Civil and Environmental Engineering, Gdańsk University of Technology, Narutowicza 11/12, 80-233 Gdańsk, Poland,
emails: erwin.wojtczak@pg.edu.pl, magdalena.rucka@pg.edu.pl

* corresponding author

Abstract

Monitoring the stiffness of adhesives is a crucial issue when considering the durability and strength of adhesive joints. While there are many studies conducted on specimens made only from adhesive, the problem of curing of an adhesive film in real joints is moderately considered. This paper presents the monitoring of stiffening of epoxy adhesive using ultrasound. Ultrasonic pulse velocity method was firstly applied for monitoring of adhesive specimens. Then, a new procedure using dispersion relations and scanning laser vibrometry was proposed for monitoring the curing process of an adhesive joint of steel plates. Both approaches gave comparable results showing the increase of the dynamic elastic modulus of adhesive in time. The study presented that the proposed procedure was capable of real-time monitoring the curing process of an adhesive layer in multi-layer systems.

Keywords

Adhesive; Curing; Ultrasound; Lamb waves; Dispersion curves; Dynamic elastic modulus

1. Introduction

The problem of structural adhesive bonding is widely considered for applications in many branches of industry, such as aviation [1,2], automotive [3,4] and civil engineering [5–7]. The use of adhesives is also essential in strengthening of existing engineering structures, e.g. bonding of FRP elements to concrete [8,9], timber [10] or steel [11,12] structures. An important issue for assessing the mechanical behaviour of adhesive is to monitor its strength and stiffness to determine the appropriate time when the destined load can be applied. Parameters, such as the modulus of elasticity, Poisson's ratio and tensile strength, are significant factors when considering the quality of the connection between bonded elements. Destructive tests ensure reliable results; however, the need for intrusion into the internal structure of a tested element is

a crucial problem. Therefore, it is preferable to use non-destructive techniques for the evaluation of adhesive behaviour. There are many methods available for non-invasive examination of adhesive joints, especially for damage identification, including ultrasonic wave-based methods [13–17], X-ray tomography [18,19] and active IR thermography [20–22].

The literature shows that the dynamic elastic parameters of various materials can be effectively determined non-invasively by ultrasonic waves, even if the specimen is in a liquid state. Qixian and Bungey [23] used compression wave ultrasonic transducers to determine the dynamic Poisson's ratio and elastic modulus of concrete slabs. Chavhan and Vyawahare [24] determined the correlation between dynamic elastic modulus and compressive strength for high strength self-compacting concrete using ultrasonic pulse analyser and compression tests. Fei et al. [25] considered P-wave and S-wave propagation in cylindrical rock samples to determine the dynamic elastic parameters. Compression tests were also done to find the correlation between static and dynamic elastic parameters. Carrillo et al. [26] conducted ultrasonic measurements to determine dynamic elastic parameters of fibre-reinforced concrete beams. The modulus of elasticity and Poisson's ratio were estimated based on the velocities of pressure and shear waves obtained from the tests with the ultrasonic pulse analyser using empirical equations. Haseli et al. [27] used ultrasonic waves to determine the dynamic modulus of elasticity for heterogeneous sandwich panels made of palm wood. Three-point static bending tests were conducted to validate the values obtained from ultrasonic tests.

The problem of determination of mechanical behaviour of epoxy adhesives in laboratory conditions and real structures has been widely considered in previous research. Michels et al. [28] considered the influence of different curing methods on the strength, stiffness and porosity characteristics for different epoxy adhesives (S&P Resin 220, Sikadur 30, Sikadur 30 LP). Tensile tests were conducted on dogbone specimens to determine the tensile strength and the elastic modulus of adhesive. The results shown that conditions of curing (temperature, type of mixing the components) have a significant impact on the identified mechanical parameters. Hu et al. [29] analysed the influence of curing history on the mechanical behaviour of epoxy adhesive (here, Araldite 2015), conducting investigations on both an adhesive specimen and real joint. A sandwich structure with a corrugated core undergone three-point bending to determine load-displacement relations (experimentally and numerically) and confirmed that the temperature is an important factor in adhesive curing. The influence of curing temperature on the physical behaviour of adhesive joints was also considered by Moussa et al. [30]. The issue of low-temperature curing of adhesives used in bridge structures was taken into analysis. It was observed that the low temperatures decelerate the curing process.

Continuous monitoring of the curing process of adhesives is also an object of interest of researchers. Lindrose [31] applied ultrasonic longitudinal and shear waves for real-time monitoring of amine-cured epoxy resin, developing a relationship between specific material parameters (e.g. attenuation, Young's and shear moduli) and time. Dixon et al. [32,33] used electromagnetic acoustic transducers to analyse the velocity of shear and compression waves in standard and rapid cure epoxy adhesives (Araldite and Permabond). The increase of shear and bulk moduli in time was observed during the curing process. Vogt et al. [34] applied ultrasonic guided waves for monitoring steel wires embedded in epoxy resin (Araldite 2012). The authors proposed attenuation and reflection coefficients as cure level indicators. Sernek and Kamke [35] used dielectric spectroscopy to analyse the curing of phenol formaldehyde adhesive film between wood plates. They concluded that the degree of cure, calculated based on the conductance of adhesive, was strongly affected by the press temperature. Jost and Sernek [36] also analysed the curing process of phenol formaldehyde adhesive, however, they revealed the relationship between bond shear strength and the degree of cure. Mascaro et al. [37] evaluated Young's modulus of epoxy adhesive cured with a polyamidoamine agent. Wedge tests with strain gauge technique were conducted as well as measurements with the ultrasonic air-coupled through-transmission method, giving comparable results. Gauthier et al. [38] used Lamb wave dispersion curves to discriminate adhesive specimens with different levels of cure. High order wave modes appeared sensitive to the epoxy conversion process, characterised by changes in bulk longitudinal and shear waves velocity. Lim et al. [39] investigated an epoxy adhesive Sikadur 330 and proposed monitoring of the curing process by the electromechanical impedance (EMI) technique. They analysed changes in the magnitude and frequency of resonance peaks of conductance signatures of a PZT patch. Measurements with wave propagation technique were also conducted to verify the results of the proposed method. Tang et al. [40] analysed the problem of analytical and numerical modelling of predicting the mechanical parameters of Sikadur 330 adhesive using guided wave propagation technique. Tensile tests and measurements of P-wave propagation were conducted to determine the tensile strength and moduli of elasticity (static and dynamic) during the curing process. Girard et al. [41] considered viscous and elastic behaviour of two-component epoxy resin (Epolam 2001/95B) under cyclic load. They analysed changes of static elastic modulus and viscosity during compression tests.

Most of the above-mentioned research on adhesives under curing has been conducted on samples prepared only from adhesive material. However, the curing conditions in the case of real adhesive joints may generally be different, thus there is the need to analyse complex, multi-

layer specimens that will allow examining the behaviour of the curing adhesive material in contact with adherends. In this paper, monitoring the curing of adhesive was considered. The aim of the study was to analyse changing the stiffness of adhesive in time. Investigations were conducted on the adhesive of significantly different geometry, i.e. adhesive samples as well as an adhesive film in a joint of two steel plates, being a simple and common type of connection. The novelty constitutes an authorial algorithm for the determination of dynamic elastic modulus based on the Lamb wave dispersion curves and statistical analysis. The proposed procedure was developed to evaluate multi-layer adhesive systems, however, it is destined to be applicable in different plate-like structures. A set of experiments verifying the results obtained by the developed algorithm was also reported.

2. A methodology of determination of elastic modulus using ultrasonic waves

The phenomenon of acoustic wave propagation in elastic media is the base for ultrasonic methods. There are two main techniques, which exploit ultrasound. The first is ultrasonic pulse velocity (UPV) method that uses bulk waves, i.e. pressure wave (longitudinal, P-wave) and shear wave (transverse, S-wave), that propagate in unrestrained media. While the values of the density and Poisson's ratio of analysed material are known, measurements of a longitudinal wave are enough to determine the elastic modulus. The velocity of the P-wave in a homogeneous isotropic elastic medium can be calculated based on the density of material ρ, dynamic elastic modulus E_d and Poisson's ratio v using the formula:

$$c_L = \sqrt{\frac{E_d\left(1-\nu\right)}{\rho\left(1+\nu\right)\left(1-2\nu\right)}}. \tag{1}$$

Assuming that analysed specimen meets the assumptions of an unbounded medium, comparison of the theoretical velocity of the P-wave with the value calculated from experimental measurements (based on the time of flight of wave t_P through the thickness of the element h) allows determining the dynamic elastic modulus of elasticity as:

$$E_d = \frac{\rho h^2\left(1+\nu\right)\left(1-2\nu\right)}{t_P^2\left(1-\nu\right)}. \tag{2}$$

Another approach is based on the guided waves, which are a special kind of acoustic waves propagating in bounded media. For example, if a medium is restrained by two parallel surfaces (e.g. a single or multi-layer thin plate) so-called Lamb waves can exist. In general, guided waves are dispersive (i.e. their characteristics are frequency-dependent) and multimodal (i.e. many symmetric and antisymmetric modes propagate for a certain frequency). These features create the opportunity for many applications of guided waves in the non-destructive

assessment of various engineering structures. Dispersion relations present the dependence of wave characteristics to the frequency and are vulnerable to any changes of parameters of analysed medium (such as elastic modulus). Thus, dispersion curves can be used for non-destructive determination of material parameters, e.g. in composites [42,43].

In this paper, a procedure of determination of the elastic modulus of adhesive based on the Lamb wave propagation method and dispersion curves is proposed. The algorithm is intended to evaluate multi-layer systems composed of thin plates bonded together using adhesive and it is desired to be applicable for different types of adhesives and adherends. A schematic diagram of the developed procedure is presented in Figure 1. The procedure consists of three paths (I, II, III). Experimental dispersion relations are determined (path I) and, independently, theoretical dispersion curves are calculated (path II).

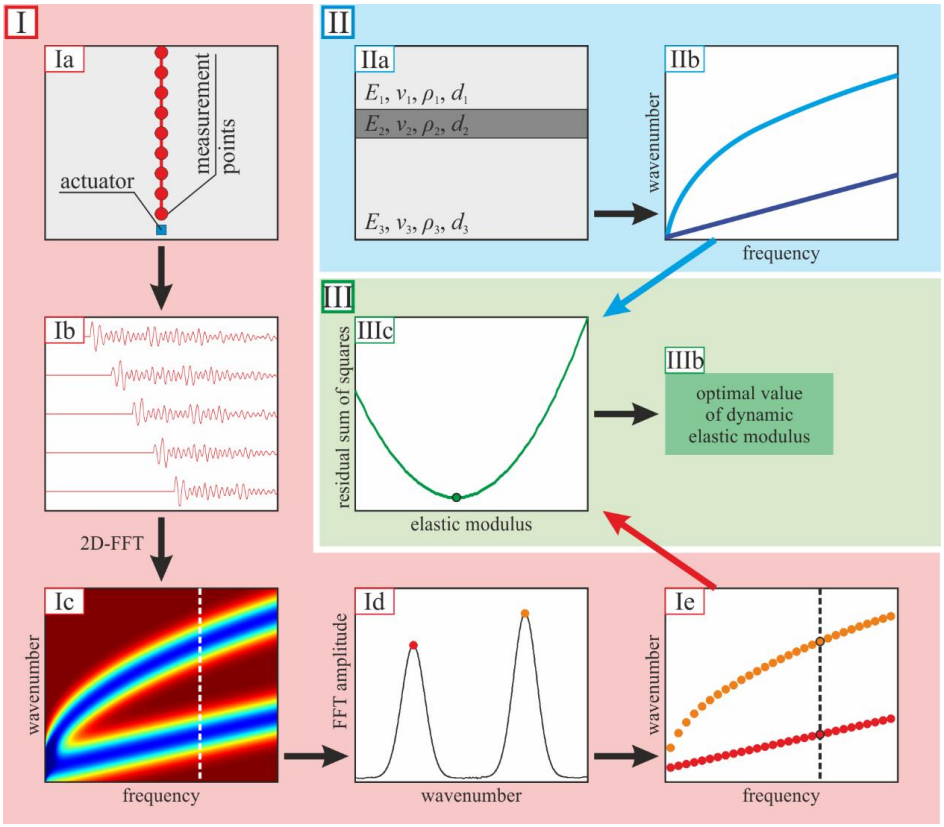

Figure 1. A schematic diagram illustrating the concept of monitoring of changes of dynamic elastic modulus in adhesively bonded plates using Lamb wave dispersion curves; I – scheme for determination of experimental dispersion curves using SLDV, II – determination of theoretical dispersion curves, III – optimization process

The first step in the experimental path is the preparation of a physical model (Ia). The measurement of time signals of propagating wave (Ib) in a set of points distributed along a straight line on analysed specimen needs to be conducted. The wavenumber-frequency relations (maps, Ic) are determined using two dimensional fast Fourier transformation (2D-FFT) [44–46] of signals recorded. To obtain dispersion curves in a wider frequency range, the measurements

should be repeated for different excitation frequencies and, if possible, different locations of an actuator. The final result is an aggregation of compound maps. Dispersion curves are then extracted from a 2D map by searching for peak values in relations between the 2D-FFT amplitude and wavenumber for each specific frequency in analysed range (Id). Each peak value is denoted as 'non-zero', whereas all remaining points are denoted as 'zero'. Extraction of all 'non-zero' points allows one to plot dispersion relations in the destined form of single curves (separate one-dimensional functions, Ie).

Theoretical models (IIa) in a probable elastic modulus range with the assumed step for an analysed frequency range are prepared. A set of theoretical curves (IIb) is calculated for prepared models. There are many methods that can be used for determination of theoretical dispersion relations, depending on the type of analysed structure. For a single layer plate made of homogeneous isotropic elastic material dispersion relations can be determined by the solution of analytical Rayleigh-Lamb frequency equations (e.g. [47]). Multi-layer plates, being much more complex media, needs the use of matrix techniques, such as transfer matrix method and global matrix method or numerical methods, e.g. semi-analytical finite element method (SAFE) [47], utilized by GUIGUW software [48].

The final path (III) is the comparison of theoretical and experimental dispersion curves based on the multiple calculation of the residual sum of squares (RSS, sum of squared residuals, IIa), being simple but very useful statistical measure. In the present work, the RSS is determined for wavenumber values obtained from the extracted experimental curve and the specific theoretical curve with respect to the formula:

$$RSS = \sum_{i=1}^{N} \left(k_{e,i} - k_{t,i} \right)^2 . \tag{3}$$

In the equation, $k_{e,i}$ and $k_{t,i}$ denote the real wavenumber values determined experimentally and theoretically, respectively, and N is the number of points in the analysed curve. The RSS calculations are repeated for a series of theoretical curves obtained for elastic modulus in a specific range, resulting with a relation between the RSS and elastic modulus. The optimal value of elastic modulus (IIb) is then determined by the minimization of the RSS function. Knowing that all wave modes can change in relation with mechanical parameters, any curve can be chosen for optimization, however, it is beneficial to analyse curve that is highly sensitive to elastic modulus value and covers wide frequency range. It is also worth noting that more than one curve can be taken into account at the same time. However this could require calculation of more than one RSS function, and, if the frequency range for both curves is not the same, determination of weights for each function could comprise complications.

3. Experimental investigations

3.1. Object of investigations

The object of the research was an adhesive Loctite Hysol 9461 (Henkel, Germany). It is a thixotropic two-component epoxy-amine resin with a volume mixing ratio of 1:1. The application of the adhesive was conducted with the dosing pistol and automatic mixing nozzle providing the homogeneity of the destined paste. Experiments were conducted on various types of specimens made of adhesive as well as on a three-layer sample composed of two steel plates joined together by an adhesive layer. Types of specimens used throughout the study are presented in Table 1. Firstly, the tests focused on the determination of dynamic elastic modulus for fully-cured adhesive using UPV and guided waves methods were performed on ten cylinders (#A1-#A10, Figure 2a) and a plate (#B, Figure 2b), all made of considered adhesive. Different types of samples were prepared to enable both measurement techniques to be used. Cylindrical specimens were made for UPV tests while the plate specimen was intended for determining dispersion curves by guided wave propagation. The dimensions of a plate were 200 *x* 100 *x* 2.55 mm^3, whereas cylinders had a height of 30 mm and a circular base with a diameter of 20 mm. Each specimen was prepared in silicone mould made of a universal two-component room temperature condensation curing silicone (type MM922).

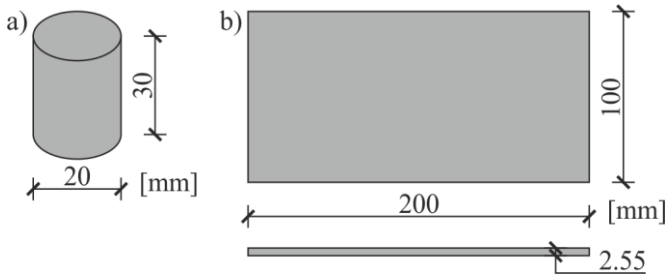

Figure 2. Adhesive specimens for initial tests: a) cylinders #A, b) plate #B

Table 1. Types of specimens examined in the research

Type	Shape	Number	Material	Testing method	Specification of tests
#A	cylinder	10	adhesive	UPV technique	single measurements on fully-cured samples
#B	plate	1	adhesive	guided wave propagation	single measurements on fully-cured samples
#C	cylinder	1	adhesive	UPV technique	multiple measurements during curing of adhesive
#D	cylinder	1	adhesive	UPV technique	multiple measurements during curing of adhesive
#E	plate	1	steel, adhesive	guided wave propagation	multiple measurements during curing of adhesive

Essential investigations, aimed at monitoring the curing process, were conducted on two adhesive cylinders (#C, #D) and a three-layer system with an adhesive film (#E). The cylinders (Figure 3a,c) had an equal height of 30 mm and different diameters: #C, d_1 = 35 mm and #D, d_2 = 20 mm. The measurements on cylinders were conducted in moulds open from both sides. A thin plastic foil was attached at the ends of moulds to prevent from leakage of adhesive. The joint #E (Figure 3b,d) consisted of two steel plates with dimensions of 200 *x* 100 *x* 2.96 mm^3 bonded by the adhesive film with a thickness of 0.38 mm. The thickness of the steel plates was determined before the joint was prepared, while the thickness of the adhesive film was the difference between the total thickness of the joint (after curing) and the thicknesses of the adherends. To prevent from debonding, the plates were treated before joint preparation with a sandpaper (type P120) and cleaned with a Loctite-7063 cleaner. All specimens (#C, #D, #E) were monitored for seven days at room temperature.

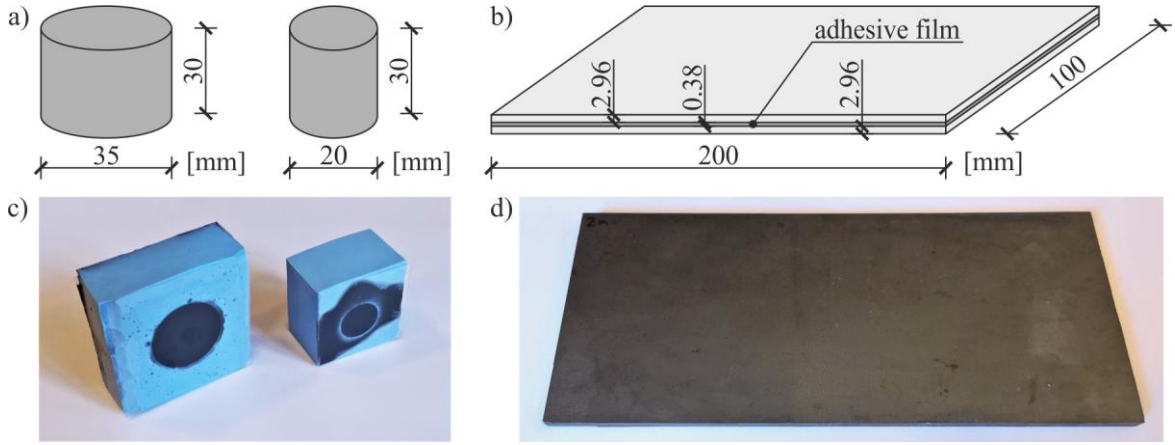

Figure 3. Specimens for monitoring the curing process: a) geometry of cylinders #C and #D, b) geometry of adhesive joint #E, c) photograph of cylinders #C and #D in silicone moulds, d) photograph of adhesive joint #E

Material properties of adhesive and steel were identified. Static tensile tests were used to determine the static modulus of elasticity and Poisson's ratio. Six steel bars with dimensions of 200 *x* 20 *x* 3 mm^3 were examined using Zwick/Roell Z100 testing machine equipped with a contacting extensometer makroXtens II WN (Zwick, Germany). Eight dogbone adhesive specimens with a length of 150 mm and an effective cross section 20 *x* 3 mm^2 were tested with Zwick/Roell Z10 machine supported with an optical videoXtens extensometer (Zwick, Germany), allowing measurements of longitudinal and transverse elongation. The results of the static tests for adhesive and steel specimens are presented in Table 2 and Table 3, respectively. The mean values of static elastic moduli for steel and adhesive were $E_{s,s}$ = 201.83 GPa and $E_{a,s}$ = 2.308 GPa, respectively, with standard deviations and coefficients of variation equal to 4.53 GPa, 2.24% (for steel) and 0.075 GPa, 3.23% (for adhesive). The mean value of Poisson's ratio for adhesive was $\nu_{a,s}$ = 0.406 (with standard deviation of 0.014 and coefficient of variation

3.39%). The Poisson's ratio for steel was assumed to be $\nu_{a,s} = 0.3$. The density was determined for both materials, independently for each set of specimens. For steel plates, it was obtained as $\rho_s = 7780.30$ kg/m^3. For adhesive plate #B, measurements gave $\rho_{a,B} = 1399.55$ kg/m^3, whereas for cylinders it was $\rho_{a,A} = 1442.08$ kg/m^3. The density obtained for each of monitored cylinders #C and #D was close to the value calculated for fully cured cylinders #A1-#A10 and equal to $\rho_{a,C} = 1459.65$ kg/m^3 and $\rho_{a,D} = 1446.58$ kg/m^3, respectively. The density of the adhesive film in joint #E was assumed to be the same as for cylinders #A1-#A10 ($\rho_{a,E} = 1442.08$ kg/m^3).

Table 2. Determination of static elastic modulus for steel bars

No	1	2	3	4	5	6
$E_{s,s}$ [GPa]	196.924	200.757	205.806	201.591	197.507	208.376

Table 3. Determination of elastic parameters for adhesive dogbone specimens

No	1	2	3	4	5	6	7	8
$E_{a,s}$ [GPa]	2.407	2.375	2.366	2.205	2.225	2.345	2.278	2.266
$\nu_{a,s}$	0.385	0.429	0.410	0.414	0.395	0.403	0.397	0.413

3.2. Experimental setup

3.2.1. Ultrasonic pulse velocity technique

Ultrasonic pulse analyser Pundit PL-200 (Proceq) equipped with transducers with a central frequency of 54 kHz was used for the measurements of time of flight of P-wave in adhesive cylinders, both fully cured (#A1-#A10) and monitored (#C, #D). The aim of the UPV tests was to provide a reference value of the dynamic elastic modulus for comparison with the results obtained from Lamb wave dispersion curves. The experimental setup is shown in Figure 4. The cylinder specimen was placed between ultrasonic transducers and a gel couplant was used between contacting faces. The wave was excited by the transmitting transducer at one side of the sample, then propagated through its thickness and received on the other side by the receiving transducer. As the result, the time of flight t_P of the excited P-wave was determined.

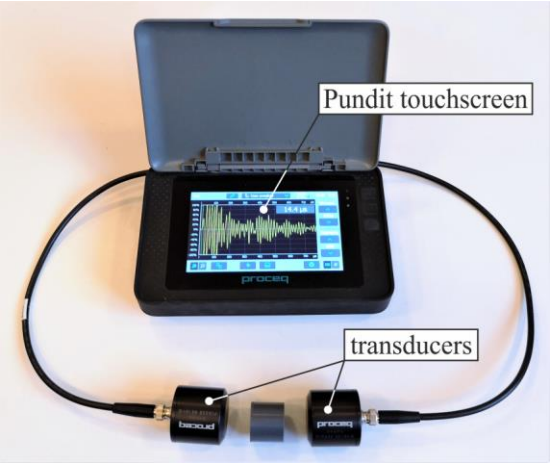

Figure 4. Ultrasonic pulse analyser setup

3.2.2. Scanning laser vibrometry

Experimental investigations consisted of measurements of Lamb waves propagating in examined specimens (fully cured adhesive plate, steel plates and the joint during the curing process). The setup used for experiments is presented in Figure 5a. The input signal was generated by the arbitrary function generator AFG 3022 (Tektronix, Inc.) with the support of the high-voltage amplifier PPA 2000 (EC Electronics). The excitation of Lamb waves was provided by the plate piezoelectric actuators NAC2024 and NAC2025 (Noliac) with dimensions of 3 x 3 x 2 mm^3 and 5 x 5 x 2 mm^3, respectively. The sensors (Figure 5b) were bonded to each specimen by petro wax 080A109 (PCB Piezotronics, Inc.). The actuators utilise the effect, that the electric field applied in parallel to the direction of spontaneous polarisation causes a vertical (thickness-wise) expansion altogether with a lateral (in plane) contraction [49]. The measurements were performed independently for two different locations of PZT actuators to induce different types of dominant waves. Firstly, the elastic waves were excited perpendicularly to the plate surface (actuator #1 in Figure 5b) inducing propagation of mainly antisymmetric modes and, then, the waves were excited in the plane of the joint (actuator #2 in Figure 5b), allowing symmetric modes to appear more explicitly.

The excitation was a single-cycle wave packet obtained by Hanning windowing of a sinusoidal burst with a central frequency of different values, consecutively, 50 kHz, 100 kHz and 150 kHz. The signals of propagating waves were acquired by a non-contact method using the scanning head of the laser vibrometer PSV-3D-400-M (Polytec GmbH) equipped with a VD-07 velocity decoder (Figure 5a). The recording equipment was synchronised with the transmission hardware. The sampling frequency of recorded signals was equal to 2.56 MHz. Each signal was averaged 20 times to improve the signal-to-noise ratio. The values of out-of-plane velocity components were acquired point by point in the 91 points distributed regularly

along the line with a length of 90 mm (Figure 5c), thus the scan resolution was equal to 1 mm. A retro-reflective sheeting was stuck on the surface of the specimen in the area of the trace line in order to improve light backscatter (Figure 5b).

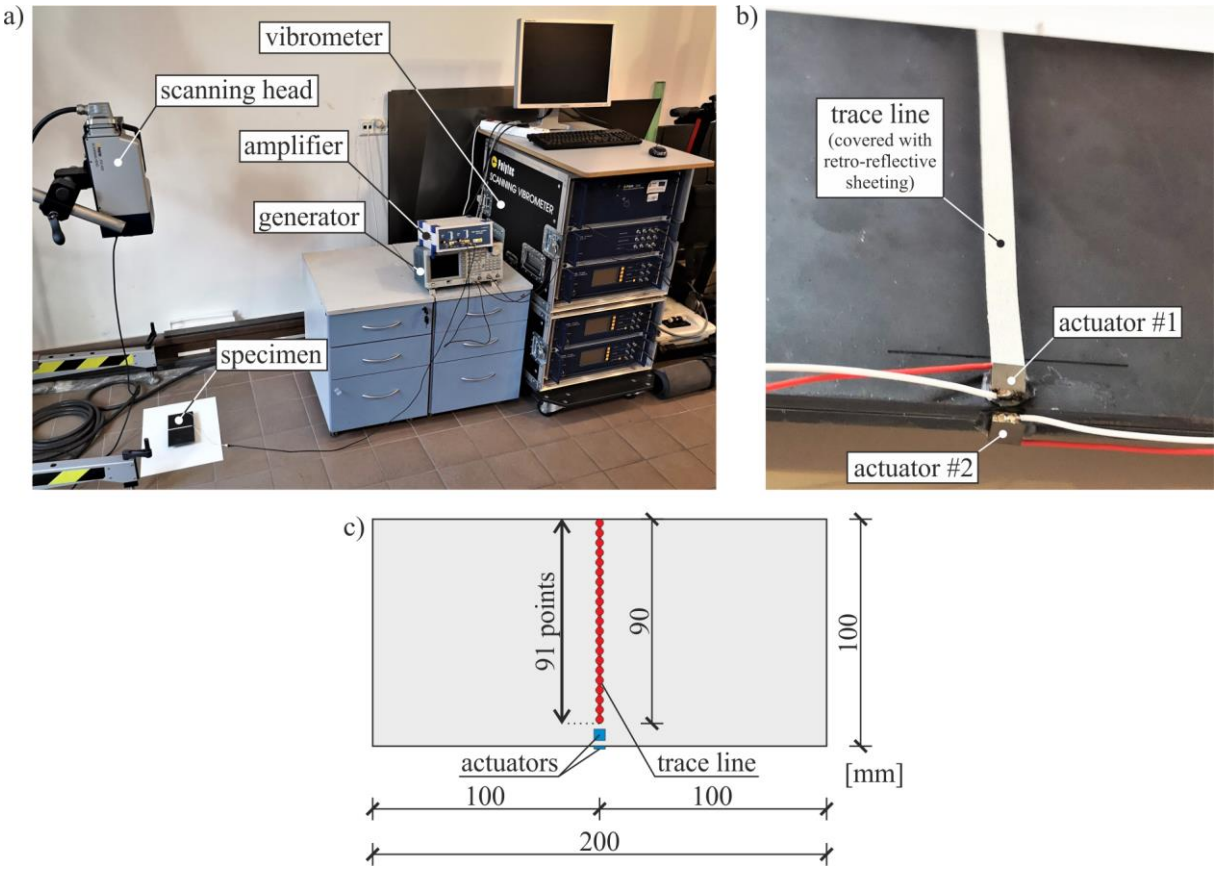

Figure 5. Scanning laser vibrometry for experimental determination of dispersion curves in plate elements: a) experimental setup, b) view of piezo actuators and trace line on a joint, c) scheme of scanning points

3.3. Monitoring of curing process

The aim of monitoring of curing process was the identification of the dynamic elastic modulus of adhesive in time with the assumption that other material parameters are constant. The duration of curing was 7 days because after this time the material was expected to be fully cured (according to producer's information sheet). The determination of the actual value of the elastic modulus (in a specific time instance) was conducted by two methods, depending on analysed specimens. First, the cylinders (#C, #D) were tested using the UPV technique. The measurements started right after the preparation of specimens, as the samples were in open moulds covered with the plastic foil on both sides (see Figure 3c). Due to a large variation in the results obtained, the time interval between two consecutive measurements was relatively small during the first day and equal to: 15 minutes (for the first 5 hours) and 30 minutes (between 6 and 16 hours of measurements). During the second and the third day of

investigations, the interval was changed to 1 hour and 2 hours, respectively. Then, measurements were taken after 3, 6 and 7 days of curing.

The adhesive joint #E of steel plates was monitored using guided wave propagation method, by means of the scanning laser vibrometer. Before joint preparation, steel plates were scanned. Then, a three-layer sample was manufactured. During each measurement, signals were registered in 91 points six times (three excitation frequencies, two actuators). Each stage of registration of 91 signals lasted about 90 seconds. The first measurement was done just after bonding. Then, during first 8 hours after bonding, measurements were repeated with different intervals equal to: 15 minutes (for the first one hour), 30 minutes (from 1 hour to 4 hours) and 60 minutes (from 4 hours to 8 hours). Then, measurements were carried out after 1, 2, 3 and finally 7 days.

4. Results and discussion

4.1. Dynamic elastic modulus for adhesive

4.1.1. Results of UPV measurements

The dynamic elastic modulus of the adhesive material was determined using both methods described in section 2. The results for adhesive cylinders (#A1-#A10) tested by the UPV method are given in Table 4. The dynamic elastic modulus was calculated based on the time-of-flight of P-wave, according to Eq. (2). The mean value of dynamic elastic modulus was calculated as $E_{a,d,\#A} = 3.678$ GPa. The standard deviation and coefficient of variation were $\sigma_E = 0.037$ GPa and $v_E = 1.01\%$, respectively. The low value of the coefficient of variation indicates the correctness of the results. The dynamic elastic modulus for the adhesive is significantly higher than the static value (a relative increase of 59.4%). For adhesives and other viscous materials, it is a commonly observed effect, resulting from the high strain rate applied to the specimens during dynamic tests (e.g. [40,50–53]).

Table 4. Determination of dynamic elastic modulus for adhesive in ultrasonic pulse analyser tests (cylinders #A1-#A10)

No	Height h [mm]	Density ρ [kg/m^3]	Time t_P [μs]	Dynamic elastic modulus E [GPa]
#A1	29.56	1440.50	12.3	3.702
#A2	29.64	1439.54	12.4	3.660
#A3	29.60	1447.38	12.3	3.730
#A4	29.57	1447.37	12.3	3.722
#A5	29.54	1445.89	12.4	3.651

#A6	29.57	1441.48	12.3	3.707
#A7	29.69	1442.37	12.4	3.680
#A8	29.50	1439.56	12.4	3.626
#A9	29.56	1435.17	12.4	3.629
#A10	29.66	1441.51	12.4	3.670

4.1.2. Results of Lamb wave propagation measurements

The dynamic elastic modulus for adhesive plate #B was obtained using dispersion relations of Lamb waves, according to the procedure described in section 2. The theoretical dispersion curves needed for comparison with experimental relations were calculated by solving Rayleigh-Lamb equations using an authorial script prepared in Matlab®. The considered range of the elastic modulus was between 3.80 and 4.20 GPa with a step of 0.01 GPa. The S0 curve was selected for analysis due to its high sensitivity to changes of the modulus of elasticity. The minimum RSS was obtained for $E_{a,d,\#B}$ = 4.03 GPa. The acquired value of the elastic modulus was compared with previously determined moduli in Table 5. It appears to be significantly higher than static one (relative difference of 74.6%) but also slightly higher than the value obtained using the UPV technique (9.6%). However, considering that the tests were conducted on significantly different specimens (cylinders vs. plate) with the use of methods based on the propagation of different types of ultrasonic waves (P-waves vs. guided Lamb waves) and by different equipment (ultrasonic pulse analyser vs. scanning laser vibrometer), the discrepancy can be considered relatively small. Based on the comparison between dynamic elastic modulus values, it can be stated that the UPV method confirms the correctness of the proposed dispersion curve-based procedure. Figure 6 shows the results of determining the dynamic elastic modulus of adhesive plate #B. The theoretical curves for the optimal value of the dynamic elastic modulus were superimposed on the experimental dispersion curves in the form of 2D FFT map. It is visible that fundamental modes A0 and S0 are clearly identifiable. Also, A1 and S1 modes propagate in the assumed frequency range; however, only A1 is moderately visible in the experimental results (S1 does not appear).

Table 5. Comparison of elastic moduli for adhesive, determined using different methods

No	Measurement technique	Type of method	Elastic modulus [GPa]
1	tensile test	static	2.31
2	UPV method	dynamic	3.68
3	guided wave propagation method	dynamic	4.03

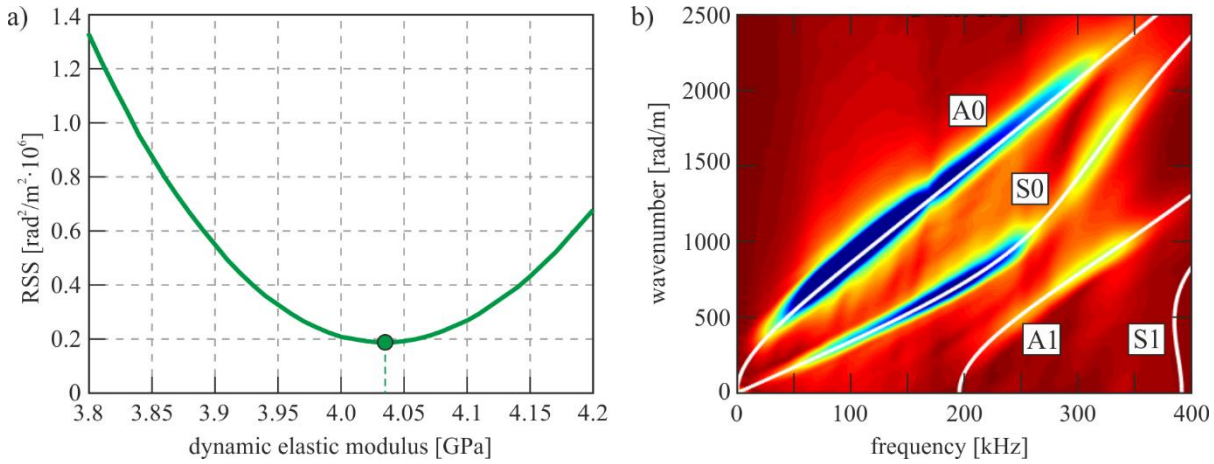

Figure 6. Determination of dynamic elastic modulus for adhesive plate #B: a) relation between RSS and elastic modulus with optimal value marked, b) experimental dispersion curves (2D FFT map) and theoretical dispersion curves from Rayleigh-Lamb equations (white lines)

4.2. Monitoring of adhesive curing

4.2.1. Monitoring of adhesive cylinders

Firstly, the results for adhesive cylinders #C and #D tested by the UPV technique are presented. Figure 7 shows the change in the dynamic elastic modulus over time using linear and logarithmic scales for the time axis. Figure 7a (with linear scaling) clearly shows that the elastic modulus increases significantly in the first curing stage (during the first day when the resin turned from paste to gel) from approximately 1.5 GPa to 3.6 GPa. At the further stage of the curing process, when the resin was solid, only a slight increase in the elastic modulus value was observed. No changes were visible between the last two measurements (with an accuracy of the equipment used), which proved that the choice of one week-lasting monitoring time was correct. Figure 7b (with logarithmic scaling) demonstrates more precisely the first stage of curing when differences between two cylinders are observable. The results for sample #C indicate that the elastic modulus increases more rapidly compared with sample #D, which may result from the geometry differences. However, the maximum values of the dynamic elastic modulus for both cylinders #C and #D were very close and equal to $E_{a,d,\#C}$ = 3.754 GPa and $E_{a,d,\#D}$ = 3.741 GPa, respectively. In addition, the obtained values are close to the mean value calculated for fully cured cylinders (#A1-#A10) equal to $E_{a,d,\#A}$ = 3.678 GPa.

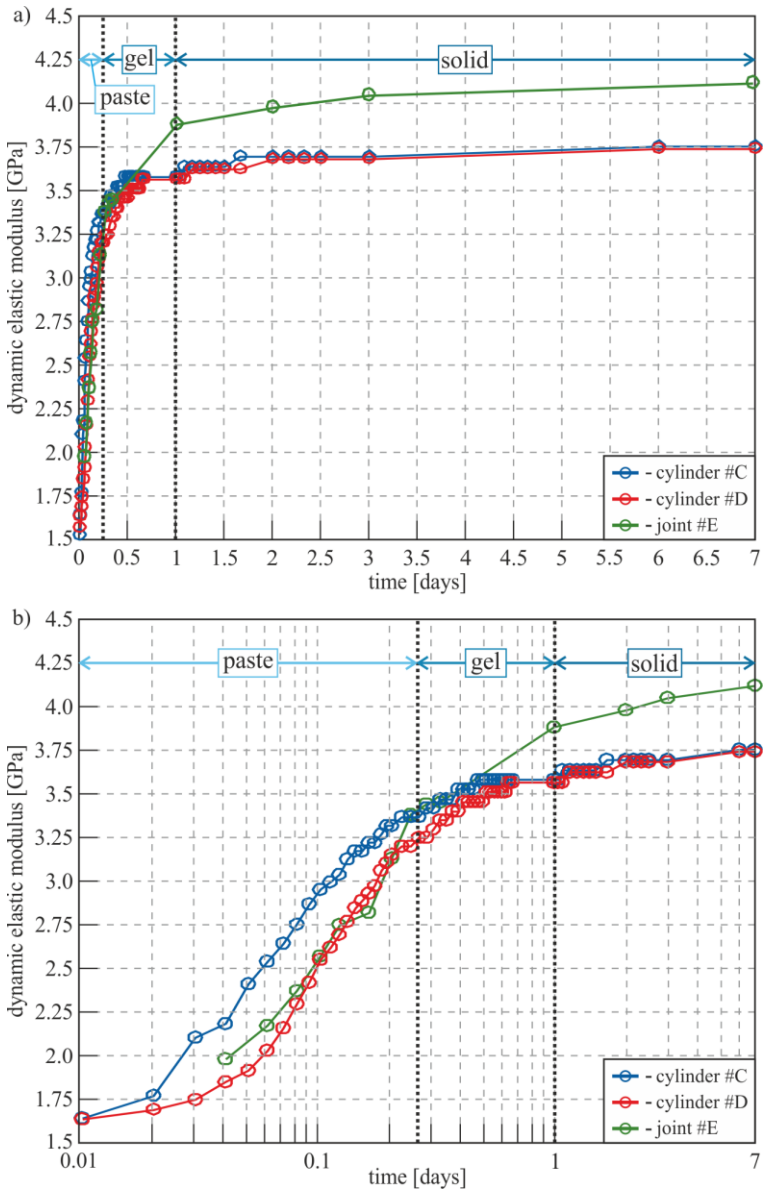

Figure 7. Monitoring of adhesive cylinders #C and #D (tested with UPV technique) and joint #E (tested with guided wave propagation technique), presenting changes in dynamic elastic modulus in time: a) linear scale, b) logarithmic scale

4.2.2. Monitoring of adhesive film in the joint

The main part of the research are the results of monitoring using scanning laser vibrometry conducted on the adhesive joint #E. The optimization algorithm was applied for both the steel plate before bonding and the three-layer specimen. In the case of the steel plate, theoretical curves (from Rayleigh-Lamb equations) were calculated in a wide range of the elastic modulus (from 190 GPa to 220 GPa with a step of 0.01 GPa). The A0 curve was chosen because the S0 curve was moderately visible (see Figure 8a) and consequently undeterminable using the proposed curve extraction algorithm. The dynamic elastic modulus obtained for steel was $E_{s,d}$ = 209.73 GPa. The value of dynamic elastic modulus was higher than the static one; however, the increase was relatively small and amounted to 3.7%.

The dynamic elastic modulus of steel was used to prepare numerical models of the joint. Calculations of theoretical dispersion relations were carried out using GUIGUW software [48]. The value of the elastic modulus of the adhesive was assumed the only variable and changed in the range from 1.00 GPa to 4.50 GPa with a step 0.01 GPa (other parameters of the joint were constant). S0 curve was chosen to the optimisation process because it was highly sensitive to changes in elastic parameters. What is more, A0 curve was moderately visible for some time instances. The curve fitting was conducted for each measurement, starting from 1 hour after preparation (S0 curve was poorly extractable for earlier measurements). Examples of curve fitting for selected time instances within seven days of curing (including measurements for a single plate) are presented in Figure 8. The figure shows theoretical dispersion curves calculated for the optimal elastic modulus superimposed on the experimental dispersion relations. The compatibility of both approaches is clearly visible. For a single plate before bonding (Figure 8a), only two fundamental A0 and S0 modes propagated in the analysed frequency range (0-400 kHz). These two modes were also visible at the initial stage of curing (Figure 8b, 15 minutes after bonding) because the adhesive was liquid and did not efficiently bond both plates. Therefore, no optimization was done in this case. As the curing process progressed, the S0 mode appeared more clearly (Figure 8c-f). It can be observed, that the curve for S0 mode shifts to the right with increasing stiffness of the joint.

To provide a qualitative measure of curing level, the results of optimal elastic modulus calculations for each analysed time instance are shown in Figure 7, together with the results obtained for cylinders #C and #D. Similarly, as in the case of monitoring cylinders, the high increase of the elastic modulus occurred during the first day of curing. After that, the dynamic elastic modulus increased slowly and obtained the value of $E_{a,d,\#E}$ = 4.12 GPa after seven days. The value was close to the one determined for adhesive plate #B in the way of dispersion curve fitting ($E_{a,d,\#B}$ = 4.03 GPa). This compatibility proved that the complexity of the plate-like sample is not significant (three-layer specimen gave similar results like a single layer plate). However, the value was slightly different from the one determined for monitored cylinders #C and #D (approximately 10%).

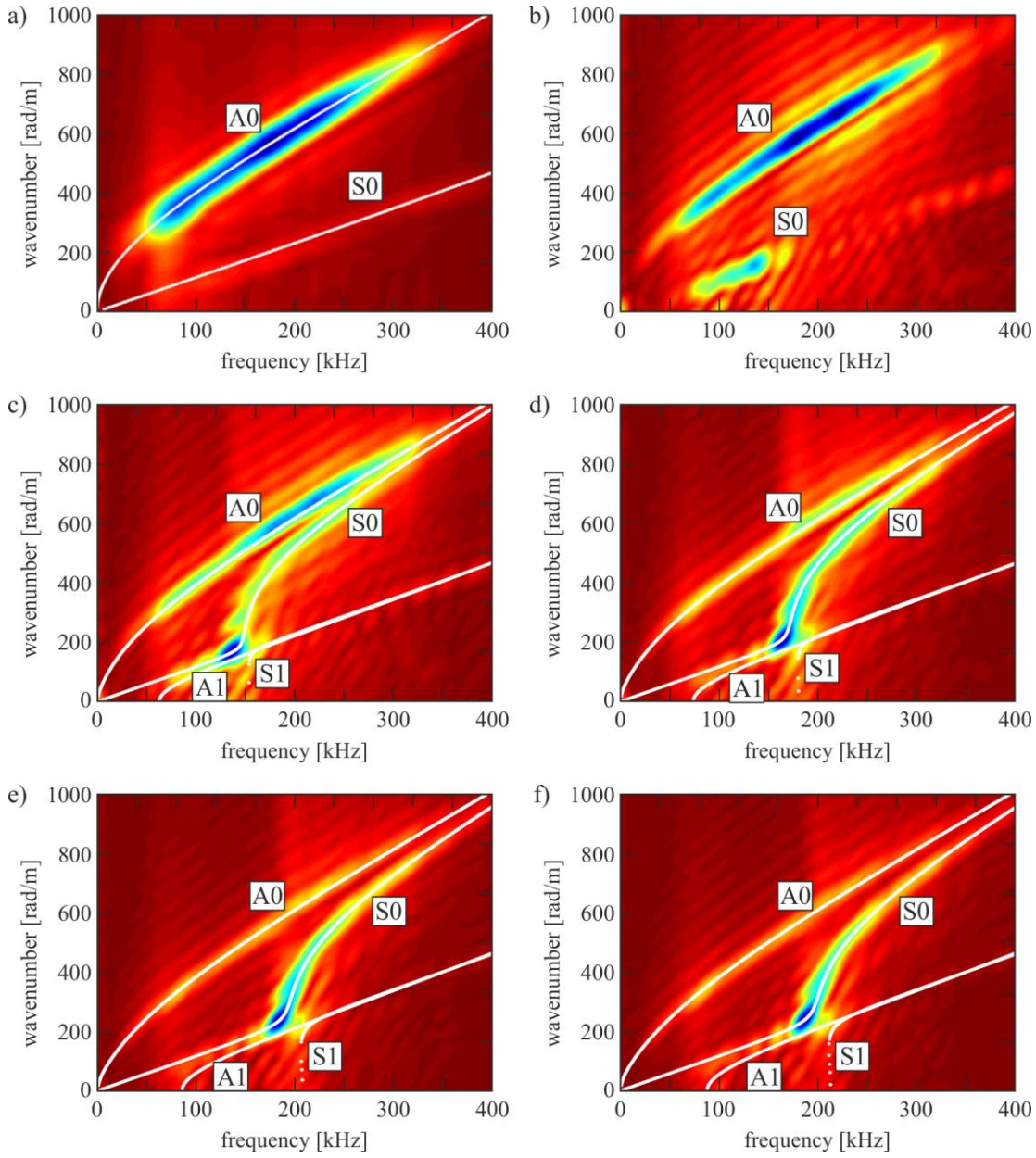

Figure 8. Examples of curve fitting for adhesive joint #E at selected time instances: a) before joining (free plate), b) 15 minutes, c) 1 hour, d) 4 hours, e) 24 hours, f) 7 days

5. Conclusions

In this paper, two ultrasonic-based methods were applied to characterize epoxy adhesive stiffness during the curing process. A procedure of determination of the elastic modulus of adhesive, based on the Lamb wave dispersion curves, was developed to evaluate multi-layer adhesive systems. A set of carefully designed experiments verifying the results obtained by the proposed procedure was also presented.

The analysis of the adhesive stiffening, observed by the increase of the dynamic elastic modulus, showed that the process was intensified in the initial part of curing. The modulus grew more slowly in the further stage and its value became almost constant after seven days of the

curing. This behaviour was observed both for cylinders (tested using the UPV technique) and the adhesive film (investigated with the Lamb waves and dispersion curves). However, the final value of the dynamic elastic modulus of adhesive obtained from both methods was slightly different. Dispersion curves fitting gave about 10% higher value comparing with the UPV measurements. The reason may be the difference in types of ultrasonic waves used (pressure and Lamb waves) and the object of measurements (cylinders and plates). Considering the complexity of plate specimens, the results obtained were compatible. Single layer and multi-layer plates (the adhesive plate and joint, both tested with the scanning laser vibrometer) gave similar values of the dynamic elastic modulus. It is also worth noting that the dynamic elastic modulus was significantly larger than the static one, regardless of the method applied. In the conducted tests, the relation was observed also for steel, but the increase was considerably smaller, thus it could be neglected.

To sum up, the proposed method can be effectively used to determine the stiffness of the adhesive in multi-layer specimens. It can be potentially applied *in situ* to monitor the curing process at selected areas of adhesive joints of real structures. Future works will focus on advancing the presented research by considering curing monitoring by other parameters, such as tensile strength.

Funding

This research did not receive any specific grant from funding agencies in the public, commercial, or not-for-profit sectors.

References

[1] A. Higgins, Adhesive bonding of aircraft structures, Int. J. Adhes. Adhes. 20 (2000) 367–376. https://doi.org/10.1016/S0143-7496(00)00006-3.

[2] F. Benyahia, A. Albedah, B.B. Bouiadjra, Analysis of the adhesive damage for different patch shapes in bonded composite repair of aircraft structures, Mater. Des. 54 (2014) 18–24. https://doi.org/10.1016/j.matdes.2013.08.024.

[3] A.F. Santos, H. Wiebeck, R.M. Souza, C.G. Schön, Instrumented indentation testing of an epoxy adhesive used in automobile body assembling, Polym. Test. 27 (2008) 632–637. https://doi.org/10.1016/j.polymertesting.2008.04.002.

[4] G. Qin, J. Na, W. Mu, W. Tan, Effect of thermal cycling on the degradation of adhesively bonded CFRP/aluminum alloy joints for automobiles, Int. J. Adhes. Adhes. 95 (2019) 102439. https://doi.org/10.1016/j.ijadhadh.2019.102439.

[5] I. Katsivalis, O. Thybo, S. Feih, M. Achintha, Failure prediction and optimal selection of adhesives for glass/steel adhesive joints, Eng. Struct. 201 (2019) 109646. https://doi.org/10.1016/j.engstruct.2019.109646.

[6] T. Tannert, A. Gerber, T. Vallee, Hybrid adhesively bonded timber-concrete-composite

floors, Int. J. Adhes. Adhes. (2019) 102490. https://doi.org/10.1016/j.ijadhadh.2019.102490.

[7] Q. Fu, L. Yan, T. Ning, B. Wang, B. Kasal, Interfacial bond behavior between wood chip concrete and engineered timber glued by various adhesives, Constr. Build. Mater. 238 (2020) 117743. https://doi.org/10.1016/j.conbuildmat.2019.117743.

[8] J.P. Firmo, M.G. Roquette, J.R. Correia, A.S. Azevedo, Influence of elevated temperatures on epoxy adhesive used in CFRP strengthening systems for civil engineering applications, Int. J. Adhes. Adhes. 93 (2019) 102333. https://doi.org/10.1016/j.ijadhadh.2019.01.027.

[9] P.L. Nguyen, X.H. Vu, E. Ferrier, Elevated temperature thermomechanical behaviour of near surface mounted CFRP reinforced concrete specimens: Effect of adhesive at concrete/CFRP interface, Eng. Struct. 197 (2019) 109361. https://doi.org/10.1016/j.engstruct.2019.109361.

[10] C. Miao, D. Fernando, M.T. Heitzmann, H. Bailleres, GFRP-to-timber bonded joints: Adhesive selection, Int. J. Adhes. Adhes. 94 (2019) 29–39. https://doi.org/10.1016/j.ijadhadh.2019.05.007.

[11] L. Ke, C. Li, N. Luo, J. He, Y. Jiao, Y. Liu, Enhanced comprehensive performance of bonding interface between CFRP and steel by a novel film adhesive, Compos. Struct. 229 (2019). https://doi.org/10.1016/j.compstruct.2019.111393.

[12] L. Ke, C. Li, J. He, S. Dong, C. Chen, Y. Jiao, Effects of elevated temperatures on mechanical behavior of epoxy adhesives and CFRP-steel hybrid joints, Compos. Struct. 235 (2020). https://doi.org/10.1016/j.compstruct.2019.111789.

[13] T.Y. Sunarsa, P. Aryan, I. Jeon, B. Park, P. Liu, H. Sohn, A reference-free and non-contact method for detecting and imaging damage in adhesive-bonded structures using air-coupled ultrasonic transducers, Materials (Basel). 10 (2017) 1–16. https://doi.org/10.3390/ma10121402.

[14] M. Rucka, E. Wojtczak, J. Lachowicz, Damage imaging in Lamb wave-based inspection of adhesive joints, Appl. Sci. 8 (2018) 1–9. https://doi.org/10.3390/app8040522.

[15] E. Wojtczak, M. Rucka, Wave frequency effects on damage imaging in adhesive joints using lamb waves and RMS, Materials (Basel). 12 (2019) 1842. https://doi.org/10.3390/ma12111842.

[16] M. Parodi, C. Fiaschi, V. Memmolo, F. Ricci, L. Maio, Interaction of Guided Waves with Delamination in a Bilayered Aluminum-Composite Pressure Vessel, J. Mater. Eng. Perform. (2019). https://doi.org/10.1007/s11665-019-04105-z.

[17] F. Nicassio, S. Carrino, G. Scarselli, Elastic waves interference for the analysis of disbonds in single lap joints, Mech. Syst. Signal Process. 128 (2019) 340–351. https://doi.org/10.1016/j.ymssp.2019.04.011.

[18] J.L. Paris, F.A. Kamke, Quantitative wood-adhesive penetration with X-ray computed tomography, Int. J. Adhes. Adhes. 61 (2015) 71–80. https://doi.org/10.1016/j.ijadhadh.2015.05.006.

[19] A. Bastani, S. Adamopoulos, T. Koddenberg, H. Militz, Study of adhesive bondlines in modified wood with fluorescence microscopy and X-ray micro-computed tomography, Int. J. Adhes. Adhes. 68 (2016) 351–358. https://doi.org/10.1016/j.ijadhadh.2016.04.006.

[20] R.C. Tighe, J.M. Dulieu-Barton, S. Quinn, Identification of kissing defects in adhesive

bonds using infrared thermography, Int. J. Adhes. Adhes. 64 (2016) 168–178. https://doi.org/10.1016/j.ijadhadh.2015.10.018.

[21] T. Lourenço, L. Matias, P. Faria, Anomalies detection in adhesive wall tiling systems by infrared thermography, Constr. Build. Mater. 148 (2017) 419–428. https://doi.org/10.1016/j.conbuildmat.2017.05.052.

[22] W.D.R. Fernando, D.A. Tantrigoda, S.R.D. Rosa, D.R. Jayasundara, Infrared thermography as a non-destructive testing method for adhesively bonded textile structures, Infrared Phys. Technol. 98 (2019) 89–93. https://doi.org/10.1016/j.infrared.2019.03.001.

[23] L. Qixian, J.H. Bungey, Using compression wave ultrasonic transducers to measure the velocity of surface waves and hence determine dynamic modulus of elasticity for concrete, Constr. Build. Mater. 10 (1996) 237–242. https://doi.org/10.1016/0950-0618(96)00003-7.

[24] P.P. Chavhan, M.R. Vyawahare, Correlation of Compressive strength and Dynamic modulus of Elasticity for high strength SCC Mixes, Int. J. Eng. Tech. Res. 3 (2015) 42–46.

[25] W. Fei, B. Huiyuan, Y. Jun, Z. Yonghao, Correlation of Dynamic and Static Elastic Parameters of Rock, Electron. J. Geotech. Eng. 21 (2016) 1551–1560.

[26] J. Carrillo, J. Ramirez, J. Lizarazo-Marriaga, Modulus of elasticity and Poisson's ratio of fiber-reinforced concrete in Colombia from ultrasonic pulse velocities, J. Build. Eng. 23 (2019) 18–26. https://doi.org/10.1016/j.jobe.2019.01.016.

[27] M. Haseli, M. Layeghi, H. Zarea Hosseinabadi, Evaluation of modulus of elasticity of date palm sandwich panels using ultrasonic wave velocity and experimental models, Meas. J. Int. Meas. Confed. 149 (2020) 107016. https://doi.org/10.1016/j.measurement.2019.107016.

[28] J. Michels, J. Sena Cruz, R. Christen, C. Czaderski, M. Motavalli, Mechanical performance of cold-curing epoxy adhesives after different mixing and curing procedures, Compos. Part B Eng. 98 (2016) 434–443. https://doi.org/10.1016/j.compositesb.2016.05.054.

[29] P. Hu, G. Akhmet, C.W. Wu, X. Han, Y.X. Chao, Y. Yu, A. Orazbayeva, Characterisation on the influence of curing history on the mechanical performance of adhesively bonded corrugated sandwich structures, Thin-Walled Struct. 142 (2019) 37–51. https://doi.org/10.1016/j.tws.2019.04.053.

[30] O. Moussa, A.P. Vassilopoulos, T. Keller, Effects of low-temperature curing on physical behavior of cold-curing epoxy adhesives in bridge construction, Int. J. Adhes. Adhes. 32 (2012) 15–22. https://doi.org/10.1016/j.ijadhadh.2011.09.001.

[31] A.M. Lindrose, Ultrasonic wave and moduli changes in a curing epoxy resin, Exp. Mech. 18 (1978) 227–232. https://doi.org/10.1007/bf02328418.

[32] S. Dixon, D. Jaques, S.B. Palmer, The development of shear and compression elastic moduli in curing epoxy adhesives measured using non-contact ultrasonic transducers, J. Phys. D. Appl. Phys. 36 (2003) 753–759. https://doi.org/10.1088/0022-3727/36/6/319.

[33] S. Dixon, D. Jaques, S.B. Palmer, G. Rowlands, The measurement of shear and compression waves in curing epoxy adhesives using ultrasonic reflection and transmission techniques simultaneously, Meas. Sci. Technol. 15 (2004) 939–947. https://doi.org/10.1088/0957-0233/15/5/023.

[34] T. Vogt, M. Lowe, P. Cawley, Cure monitoring using ultrasonic guided waves in wires, J. Acoust. Soc. Am. 114 (2003) 1303–1313. https://doi.org/10.1121/1.1589751.

[35] M. Sernek, F.A. Kamke, Application of dielectric analysis for monitoring the cure process of phenol formaldehyde adhesive, Int. J. Adhes. Adhes. 27 (2007) 562–567. https://doi.org/10.1016/j.ijadhadh.2006.10.004.

[36] M. Jost, M. Sernek, Shear strength development of the phenol-formaldehyde adhesive bond during cure, Wood Sci. Technol. 43 (2009) 153–166. https://doi.org/10.1007/s00226-008-0217-2.

[37] B. Mascaro, M.K. Budzik, M. Castaings, J. Jumel, M.E.R. Shanahan, Evaluation of adhesive bond Young's modulus during crosslinking using a mechanical method and an ultrasound method, in: J. Phys. Conf. Ser., 2012. https://doi.org/10.1088/1742-6596/353/1/012006.

[38] C. Gauthier, D. Leduc, J. Galy, M.E. Elkettani, J.L. Izbicki, Discrimination of epoxy curing by high lamb modes order, Phys. Procedia. 70 (2015) 300–304. https://doi.org/10.1016/j.phpro.2015.08.159.

[39] Y.Y. Lim, Z.S. Tang, S.T. Smith, Piezoelectric-based monitoring of the curing of structural adhesives: A novel experimental study, Smart Mater. Struct. 28 (2019). https://doi.org/10.1088/1361-665X/aaeea4.

[40] Z.S. Tang, Y.Y. Lim, S.T. Smith, I. Izadgoshasb, Development of analytical and numerical models for predicting the mechanical properties of structural adhesives under curing using the PZT-based wave propagation technique, Mech. Syst. Signal Process. 128 (2019) 172–190. https://doi.org/10.1016/j.ymssp.2019.03.030.

[41] M. Girard, M. Péron, A. Uguen, P. Casari, F. Jacquemin, A simple characterization methodology for the identification of the visco-elastic behavior of thermoset adhesives during cure, Appl. Adhes. Sci. 8 (2020). https://doi.org/10.1186/s40563-020-00125-4.

[42] W.H. Ong, N. Rajic, W.K. Chiu, C. Rosalie, Determination of the elastic properties of woven composite panels for Lamb wave studies, Compos. Struct. 141 (2016) 24–31. https://doi.org/10.1016/j.compstruct.2015.12.017.

[43] A. Gallina, L. Ambrozinski, P. Packo, L. Pieczonka, T. Uhl, W.J. Staszewski, Bayesian parameter identification of orthotropic composite materials using Lamb waves dispersion curves measurement, J. Vib. Control. 23 (2017) 2656–2671. https://doi.org/10.1177/1077546315619264.

[44] D.N. Alleyne, P. Cawley, A 2-dimensional Fourier transform method for the quantitative measurement of Lamb modes, Proc. IEEE Ultrason. Symp. 2 (1990) 1143–1146. https://doi.org/10.1109/ULTSYM.1990.171541.

[45] M.S. Harb, F.G. Yuan, A rapid, fully non-contact, hybrid system for generating Lamb wave dispersion curves, Ultrasonics. 61 (2015) 62–70. https://doi.org/10.1016/j.ultras.2015.03.006.

[46] C. Gauthier, J. Galy, M. Ech-Cherif El-Kettani, D. Leduc, J.L. Izbicki, Evaluation of epoxy crosslinking using ultrasonic Lamb waves, Int. J. Adhes. Adhes. 80 (2018) 1–6. https://doi.org/10.1016/j.ijadhadh.2017.09.008.

[47] J.L. Rose, Ultrasonic Guided Waves in Solid Media, Cambridge University Press, New York, 2014. https://doi.org/10.1017/CBO9781107273610.

[48] P. Bocchini, M. Asce, A. Marzani, E. Viola, Graphical User Interface for Guided Acoustic Waves, J. Comput. Civ. Eng. 25 (2011) 202–210.

https://doi.org/10.1061/(ASCE)CP.1943-5487.0000081.

[49] V. Giurgiutiu, Structural Health Monitoring with Piezoelectric Wafer Active Sensors, Elsevier, 2008.

[50] M. Braem, P. Lambrechts, G. Vanherle, V. Van Doren, M. Braem, The Impact of Composite Structure on Its Elastic Response, J. Dent. Res. 65 (1986) 648–653. https://doi.org/10.1177/00220345860650050301.

[51] J. Sabbagh, J. Vreven, G. Leloup, Dynamic and static moduli of elasticity of resin-based materials, Dent. Mater. 18 (2002) 64–71. https://doi.org/10.1016/S0109-5641(01)00021-5.

[52] G.C. Jacob, J.M. Starbuck, J.F. Fellers, S. Simunovic, R.G. Boeman, Strain rate effects on the mechanical properties of polymer composite materials, J. Appl. Polym. Sci. 94 (2004) 296–301. https://doi.org/10.1002/app.20901.

[53] M. Ciccotti, R. Almagro, F. Mulargia, Static and Dynamic Moduli of the Seismogenic Layer in Italy, 37 (2004) 229–238. https://doi.org/10.1007/s00603-003-0019-7.